Modelling Retinal Vessel Flicker Response

András M Joó[1,5], Anikó Ekárt[2], Emily Scarpello[1], Konstantin Gugleta[3], Selim Orguel[3], Leopold Schmetterer[4], and Doina Gherghel[1]

[1]Vascular Research Laboratory, School of Life & Health Sciences, Aston University
[2]School of Engineering & Applied Science, Aston University
[3]Augenklinik, Universitätsspital, Basel
[4]Nanyang Tech University, Lee Kong Chian School of Medicine, Singapore
[5]Sapientia, Hungarian University of Transylvania

May 20, 2019

We propose a parsimonious mathematical model for the human retinal vessel flicker response. The model is derived from data recorded by Dynamical Vessel Analyzer (DVA, Imedos GMBH, Germany).

Keywords: retinal vessel analysis, dynamical systems.

Introduction

DVA is a commercially available retinal vessel analyzer capable of continuous measurement of retinal vessel diameters and thus, indirectly approximating the ocular blood flow [9]. The retinal vessel diameters have been shown to be correlated with various biomarkers and pathologies (e.g. age, gender, diabetes, glaucoma, etc).

While modeling the ocular blood flow has an extensive literature [8], modeling the retinal flicker response, as recorded by the DVA, is missing. This paper is an attempt to fill this gap by proposing first and second order difference equation models. The models are compared along their modeling power, easiness of interpretation, speed and noise sensitivity.

The rationale is the following: modeling serves as a feature extraction procedure which maps high dimentional measurements to low dimensional model parameters (2D, or 4D in our case). These, in turn can subsequently be leveraged in visualisation, clustering and / or classification methods.

Prior work

Studies related to our work has been done along two distinct dimensions: (1) mathematical modeling of ocular blood flow and (2) description of DVA, studies on reproducibility and examining the linkage between the different pathologies and DVA.

Mathematical models for the ocular blood flow have been proposed on different levels: (a) modeling vascular geometries [8] and mechanical properties of arteries [17], (b) modeling the dynamics of the retinal blood flow [3, 1, 2], (c) modeling the retinal blood flow auto-regulation [7, 12, 4], and (d) modeling the molecular interactions [29, 23, 28].

DVA has been shown to be a reliable way of measuring retinal vessel diameters [9]. Several studies using DVA found correlation between the retinal flicker response and lifestyle [15, 16], age and blood pressure [24], diabetes [10, 21], glaucoma [11], obesity [19] and gender differences [27].

Data source

The DVA measurement reflects the evolution of the diameters of one or more retinal vessel segments during a 350 seconds examination using a common protocol: a 50 s baseline diameter measurement under still illumination, followed by three successive flicker cycles. Each flicker cycle consists of a 20 s stimulation using a 12.5 Hz flicker and an 80 s recovery period [14]. The DVA assumes the Gullstrand eye model [13], and as the result of the examination outputs a pair of 350-element real-valued vectors corresponding to 1 Hz artery and vein diameter readings (in μm). For a comprehensive description of the recording procedure the reader is referred to [9].

Preprocessing

The DVA measurement is prone to errors from several error sources, resulting in missing or noisy diameter values [9]. In order to avoid interference with the modeling algorithm ref! we limit ourselves to only three preprocessing steps: (a) approximating missing diameter readings using linear interpolation, (b) discarding vessels responses with proportion of missing values larger than an arbitrarily fixed threshold, 20%, and (c) normalizing the individual diameter readings to zero mean and unit variance. The preprocessing leaves 4627 measurements out of 5620, belonging to 2177 individual patients.

When multiple measurements per examination are available[1] the best artery-vein pair $(\mathbf{a}_i, \mathbf{v}_j)$ which is the most representative for the given measurement is selected (Figure 1). The selection is performed so that Euclidean norms $|\mathbf{a}_i - \mathbf{A}|$ and $|\mathbf{v}_j - \mathbf{V}|$ are minimal, where $(\mathbf{A}, \mathbf{V})$ is the ideal artery and vein response pair defined as the *golden average*. The golden average was calculated by averaging all vessel responses from all recorded patients that are marked as low-noise and healthy

[1] A relatively new feature of the DVA software.

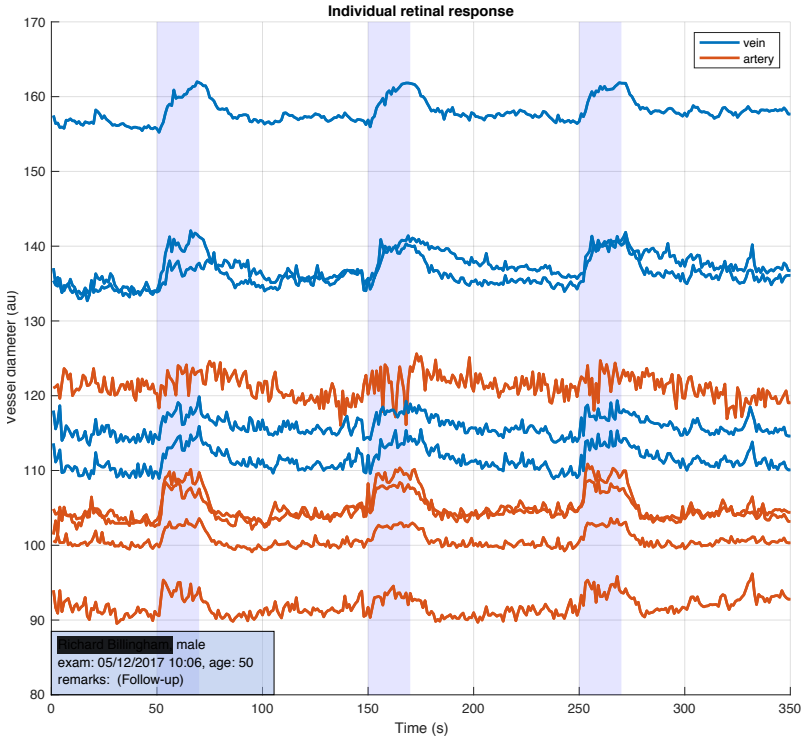

Figure 1: Sample DVA measurement of a 50-year-old male showing the evolution of diameter of five artery and five vein segments (shown in red and blue) during a 350s examination. The vessel diameter is determined from the logarithmized ratio of the intensities of the vessel-free environment of the blood vessel and of the blood vessel [14]. Vessels dilate during flicker stimulation (light blue stripes) and constrict afterwards.

by an independent medical expert. These will also serve as reference points during visualization in the absence of a ground-truth (Figure 2).

Modeling the vessel flicker response

The flicker response is correlated with the patient's age, gender, lifestyle, ethnicity and medical history [21, 27, 19, 16]. Considering all these parameters is out of the scope of this paper (even if they are available[2]) and the vessel flicker response model we build is based exclusively on the DVA measurement data.

In this context we assume that the retinal flicker response can be described by a dynamical system, where the current vessel diameter x_t depends on (a) the previous diameter values $x_{t-1}, x_{t-2}, \ldots$ and (b) the current and previous values of the flicker signal $u_t, u_{t-1}, \ldots$. We further assume that the true diameter values x_t are contaminated by some additive and unknown measurement noise

[2] Age and gender data is available for all patients. Lifestyle, ethnicity and medical history, however, is scarce.

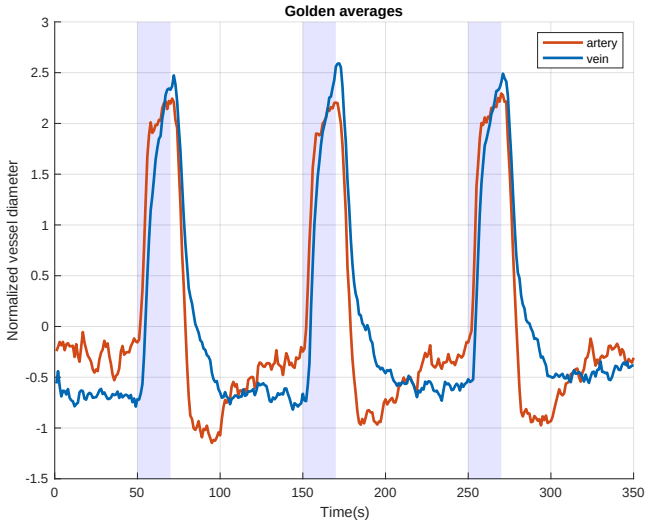

Figure 2: Normalized average of a set of good quality, hand picked arteries and veins, called golden averages.

η_t, therefore cannot be observed directly. What is observed are the *diameter readings* denoted by y_t, that is

$$y_t = x_t + \eta_t. \tag{1}$$

We define the flicker signal's value at time step t, as

$$u_t = \begin{cases} 1, \text{ if } 50 + n < t \leq 70 + n, n \in \{0, 100, 200\} \\ 0, \text{ otherwise.} \end{cases} \tag{2}$$

Consequently, the modeling problem can be formulated as the identification of a function $\Theta(\vec{x}_t, \vec{u}_t)$ so that

$$x_t = \Theta(\vec{x}_t, \vec{u}_t), \tag{3}$$

where $\vec{x}_t \equiv (x_{t-1}, x_{t-2}, \ldots x_{t-m})$ and $\vec{u}_t \equiv (u_t, u_{t-1}, \ldots u_{t-n-1})$ are vectors in the delay embedding space. After choosing a suitable form for Θ, Equation 3 is usually solved [20] using least squares by minimizing the one-step-ahead prediction error

$$\sum_t (x_{t+1} - \Theta(\vec{x}_t, \vec{u}_t))^2 \to \min. \tag{4}$$

As we do not have access to the true vessel diameter values x_t, but to diameter readings y_t, we will approximate the system dynamics by minimizing

$$\sum_t (y_{t+1} - \Theta(\vec{y}_t, \vec{u}_t))^2 \to \min, \tag{5}$$

To tackle the error-in-variables problem [18] we will consider an alternative approach as well: performing a full simulation of the response curve starting from some predefined initial values $z_1, z_2, \ldots z_m$ and minimizing the Euclidean distance between the simulated vessel response and the diameter readings, that is

$$\sum_t (y_t - z_t)^2 \to \min, \tag{6}$$

where

$$z_t = \begin{cases} c_t \in \mathbb{R}, \text{ if } t \leq m \\ \Theta(\vec{z}_t, \vec{u}_t) \text{ otherwise.} \end{cases} \tag{7}$$

In the following we will refer to the one-step-ahead prediction minimization as method P and the full simulation minimization as method S.

Physical and biological systems usually exhibit dynamics with relatively few terms [6, 26] therefore we will consider dynamical systems which can be described by first or second order difference equations.

First order dynamics

The simplest difference equation that includes both the vessel response and the flicker signal is

$$\Theta(\vec{y}_t, \vec{u}_t) \equiv \alpha y_{t-1} + \beta u_t, \text{ where } \alpha, \beta \in \mathbb{R}. \tag{8}$$

Using method P (as per Equation 5) to find the corresponding α, β and γ values is equivalent to solving the following overdetermined linear system:

$$\begin{bmatrix} y_2 \\ y_3 \\ \vdots \\ y_N \end{bmatrix} = \begin{bmatrix} y_1 & u_2 \\ y_2 & u_3 \\ \vdots & \vdots \\ y_{N-1} & u_N \end{bmatrix} \begin{bmatrix} \alpha \\ \beta \end{bmatrix}. \tag{9}$$

Calculating α, β and z_1 using method S (as per Equation 6) requires numerical optimization. We used an interior-point algorithm [5] as implemented in MATLAB's `fmincon` function with random restarts.

The optimal shift

The normalization during the preprocessing phase scales each measurement signal to unit variance and shifts it vertically to zero mean. The vertical shift influences the modeling error and the

zero meanness almost always results in suboptimal modeling error. A simple modification to Equation 8 allows the inclusion of the optimal shift (denoted as γ):

$$y_t - \gamma = \alpha(y_{t-1} - \gamma) + \beta u_t \Leftrightarrow \tag{10}$$

$$y_t = \alpha y_{t-1} + \beta u_t + (1-\alpha)\gamma. \tag{11}$$

The numerical optimization for method S can be readily adjusted to include γ as per Equation 11, while method P changes into solving the following linear system:

$$\begin{bmatrix} y_2 \\ y_3 \\ \vdots \\ y_N \end{bmatrix} = \begin{bmatrix} y_1 & u_2 & 1 \\ y_2 & u_3 & 1 \\ \vdots & \vdots & \vdots \\ y_{N-1} & u_N & 1 \end{bmatrix} \begin{bmatrix} \alpha \\ \beta \\ (1-\alpha)\gamma \end{bmatrix}. \tag{12}$$

Comparison of method S and method P

The two methods result in different set of parameters and different error values (see Figure 3). To no surprise in over 99.98% of the cases method P was found better in minimizing the prediction error and method S was better in minimizing the simulation error (see Table 1 for a summary).

Table 1: Comparison of simulation and prediction errors for method S and method P. Values reflect the average difference one method is better than the other.

	arteries	veins
simulation error, method $S \gg$ method P	8.25%	13.11%
prediction error, method $P \gg$ method S	6.94%	5.92%

Response to trend

Certain measurements have a partial trend component. While this might have physiological causes, empirical evidence shows that this is a specific measurement error[3].

One of the differences in method S and method P is their response to trends present in the data: while method S captures the trend, method P totally ignores it (see Figure 4d). In the absence of the cause of the trend it is not possible to assess which approach is more desirable and whether a de-trending preprocessing step (e.g. by subtracting a low-order regression polynomial) would be adequate.

[3] Usually occurs when, during the measurement, the patient gradually moves their forehead backwards from the fixating band or moves their chin from the support (both parts of the DVA machine) in a more comfortable position.

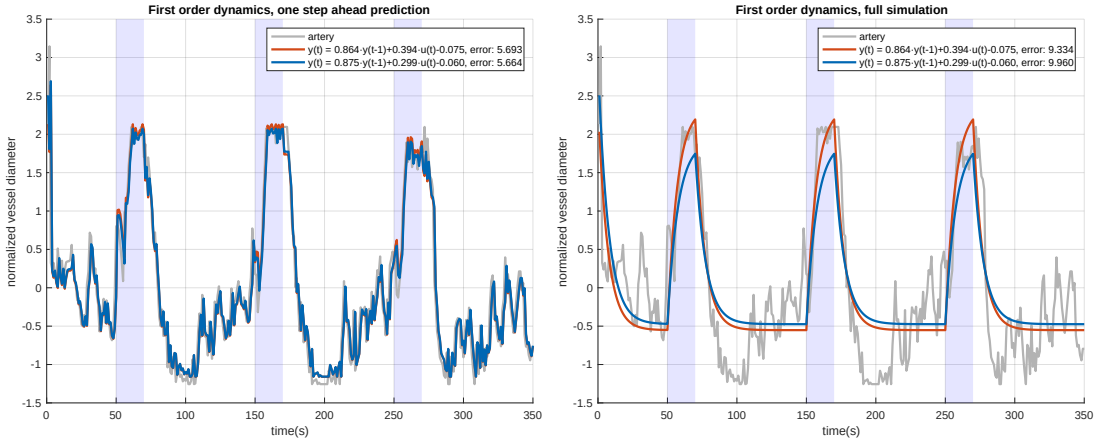

(a) One-step-ahead prediction.

(b) Full simulation.

Figure 3: Comparison of method S (red curve) and method P (blue curve) for first order dynamics for an arbitrary artery (gray curve). The two methods result in different set of parameters but similar dynamics and comparable error values.

Notes on first order dynamics

Equation 8 is a linear time-invariant (LTI) system. Its transfer function is given by

$$H(z) = \frac{Y(z)}{U(z)} = \frac{\beta}{1 - \alpha z^{-1}}, z \in \mathbb{C}. \tag{13}$$

Using the inverse z-transform this translates into the following impulse function:

$$h(n) = \beta\alpha^n, \ \forall n \in \mathbb{N}_+. \tag{14}$$

The impulse response completely characterizes the LTI system [25]. Taking the convolution of the impulse response h with an arbitrary input signal q results in the model output[4]. There are few noteworthy observations regarding coefficients α and β:

- α must be in the $(0,1)$ interval: if α is negative, then the impulse response oscillates with the parity of n; if α is zero, or one the impulse response is constant; if α is larger than 1, then the impulse response diverges; none of these are anatomically plausible.
- Negative β values equate with 'upside down' responses, i.e. they model vasonstriction instead of vessel dialtion. These happen as abnormal vessel reactions[5] or as an artefact of a noisy measurement.
- Zero or close to zero β values result in small amplitude responses.
- Apart from a few cases, all (α, β) are within the unit circle with center $(1,0)$, more precisely within the circle's sector defined by $\left|\frac{\beta}{\alpha - 1}\right| < 1$. While the former is due to the normalization, we are unsure about the latter.

[4] This makes measurements recorded with different protocols comparable.
[5] Although in vitro some vessels react with vasoconstriction, see [22].

- Measurements close to the golden average are characterized by $\beta \approx 1 - \alpha$. no idea why

The major limitation of the first order dynamics is that it cannot capture the negative overshoot and recovery phase (i.e. the ≈50s interval immediately after the flicker) irrespective of the coefficient values (see Figure 3b).

Visualization

Despite its limitations, the first order model has an important application in visualizing the model parameter space. Considering only parameters α and β, modeling can be thought as a mapping of the measurement space ($\subset \mathbb{R}^{350}$) onto the parameter space ($\subset \mathbb{R}^2$). The plot can be enhanced if the points are colored based on the golden average: the smaller the distance of the arterial measurement to the golden average, the cooler the corresponding point's color. Figure 4 shows the colored mapping of all arterial measurements using the two methods; method P provides a smoother transition between the measurements which are close to the golden average and those far from it(see Figure 4a).

Figure 4b also reveals that for a number of S models α is larger than one, despite the theory. Upon inspection it turned out that this also due to trending (see Figure 5).

Second order dynamics

To capture the negative overshoot and recovery phases we propose the following second order difference equation:

$$\Theta(\vec{y}_t, \vec{u}_t) \equiv \alpha_1 y_{t-1} + \alpha_2 y_{t-2} + \beta_1 u_t + \beta_2 u_{t-1} \text{ where } \alpha_1, \alpha_2, \beta_1, \beta_2 \in \mathbb{R}. \tag{15}$$

Similarly to the first order case, if the vessel data is not optimally shifted, the equivalent non-homogeneous equation can be used:

$$\Theta(\vec{y}_t, \vec{u}_t) \equiv \alpha_1 y_{t-1} + \alpha_2 y_{t-2} + \beta_1 u_t + \beta_2 u_{t-1} + \gamma(1 - \alpha_1 - \alpha_2) \text{ where } \gamma \in \mathbb{R}. \tag{16}$$

Without the loss of generality in the following we will assume that all vessel data has been shifted optimally prior modeling and will work only with Equation 15.

Comparison of method S and method P

Calculating the coefficients with method P requires solving the following overdetermined linear system:

$$\begin{bmatrix} y_3 \\ y_4 \\ \vdots \\ y_N \end{bmatrix} = \begin{bmatrix} y_2 & y_1 & u_3 & u_2 \\ y_3 & y_2 & u_4 & u_3 \\ \vdots & \vdots & \vdots & \vdots \\ y_{N-1} & y_{N-2} & u_N & u_{N-1} \end{bmatrix} \begin{bmatrix} \alpha_1 \\ \alpha_2 \\ \beta_1 \\ \beta_2 \end{bmatrix}. \tag{17}$$

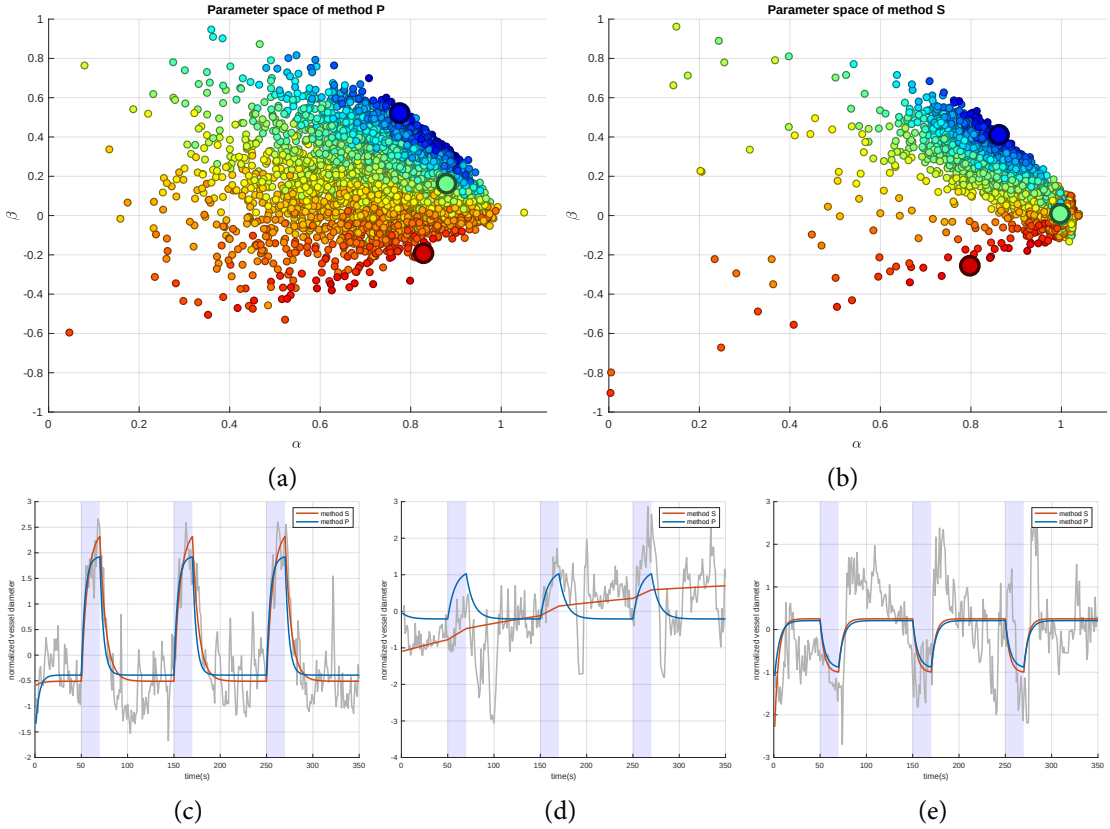

Figure 4: Parameter space of methods P and method S based on 4627 arterial measurements (first row, Figure 4a and Figure 4b). A dot with coordinates (α, β) represents a model of form $\alpha y_{t-1} + \beta u_t + \gamma$. Dots are colored according to the Euclidean distance of the arterial response to the golden average. Three measurements of increasing goodness have been highlighted in the second row: the first (Figure 4c) belongs to a 49-year-old male, the second (Figure 4d) to a 19-year-old female and the third (Figure 4e) to a 76-year-old female.

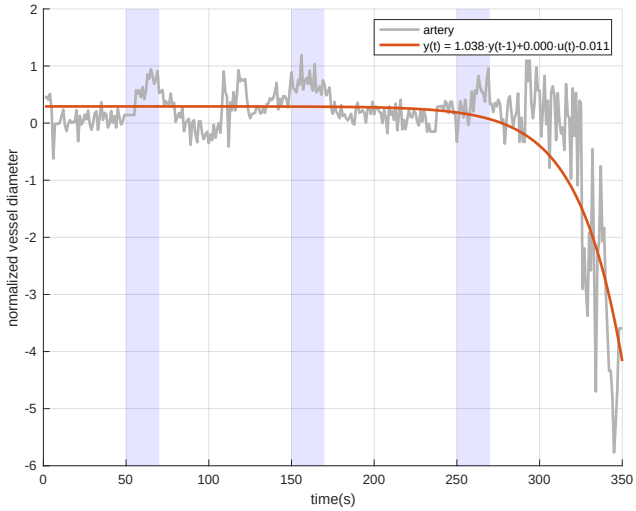

Figure 5: Strong downwards trend at the end of the measurement, possibly caused by patient movement, resulting in above unit α value in method *S*.

As for method *S*, similar to the first order dynamics, the numerical optimization needs to find coefficients $\alpha_1, \alpha_2, \beta_1, \beta_2$ and the initial values z_1 and z_2.

The outcome of the two methods for an arbitrary artery is shown in Figure 6. Please note that method *P* has a serious shortcoming: it still fails to capture the overshoot and recovery phases Figure 6b. The problem lies in the noise contaminating the arterial recordings; method *P is* capable of recovering the model coefficients from artificially generated arterial responses (using Equation 15) if the additive Gaussian 'measurement' noise is kept on very low levels, $\sigma \leq 10^{-2}$.

The comparison of the two methods considering the whole set of measurements further reveals that the addition of extra coefficients (i.e. α_2 and β_2) makes the two methods even more specialized compared to the first order case (see Table 2).

Table 2: Comparison of simulation and prediction errors for method *S* and method *P*. Values reflect the average difference one method is better than the other.

	arteries	veins
simulation error, method $S \gg$ method P	21%	22.1%
prediction error, method $P \gg$ method S	41.9%	40.6%

Simplification

The parameter space of method *S* (for the pairwise plots see Figure 7) does not provide a straightforward interpretation. What is striking, however, is the strong negative correlation between α_1 and α_2, and β_1 and β_2 (-0.9867 and 0.9723, respectively). This suggests that Equation 15 may be

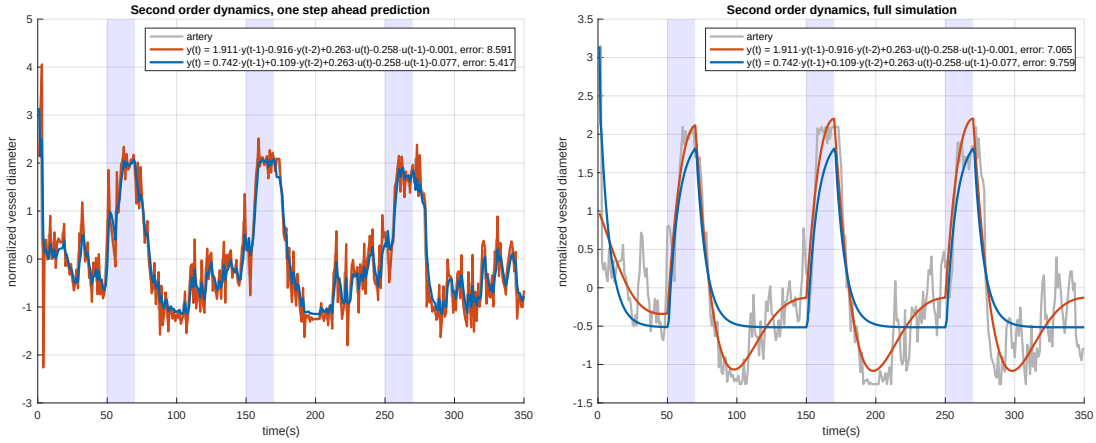

(a) One-step-ahead prediction.

(b) Full simulation.

Figure 6: Comparison of method S (red curve) and method P (blue curve) for second order dynamics for an arbitrary artery (gray curve). Method P cannot capture the negative overshoot and recovery phases.

overly complicated and a simpler expression may suffice. While $\beta_1 = \beta_2$ can be included verbatim in the new recursion, setting $\alpha_2 = 1 - \alpha_1$ would degenerate Equation 15 to a first order difference equation. The simplified formula we propose therefore is

$$\Theta(\vec{y}_t, \vec{u}_t, c_1, c_2) \equiv \alpha y_{t-1} + (c_1\alpha + c_2) y_{t-2} + \beta u_t - \beta u_{t-1}, \tag{18}$$

where real constants c_1 and c_2 are *characteristics of the method*, rather than the individual models. The optimal values for c_1 and c_2 in least squares terms can be calculated solving

$$\begin{bmatrix} \alpha_2^1 \\ \alpha_2^2 \\ \vdots \\ \alpha_2^M \end{bmatrix} = \begin{bmatrix} \alpha_1^1 & 1 \\ \alpha_1^2 & 1 \\ \vdots & \vdots \\ \alpha_1^M & 1 \end{bmatrix} \begin{bmatrix} c_1 \\ c_2 \end{bmatrix}, \tag{19}$$

where the values for α_1^k and α_2^k are provided by method S for the different measurements $k = 1 \ldots M$. Up to 4 degrees precision c_1 and c_2 were found to be -0.9913 and 0.9801 for arteries, and -0.9954 and 0.9899 for veins. An example of how the simplified method (we shall refer to it as S_2 in the following) models an arbitrary artery and vein is shown in Figure 8.

Replacing β_2 with $-\beta_1$ comes with a small increase (2.17% for arteries and 2.3% for veins) in the average modeling error, considering the modeling error of method S as the reference value. The two simplifications together increase the average modeling error by 10.1% for arteries and by 8.8% for veins.

Running on a subset of the patients, e.g. on those marked as healthy would probably yield different values. To discuss.

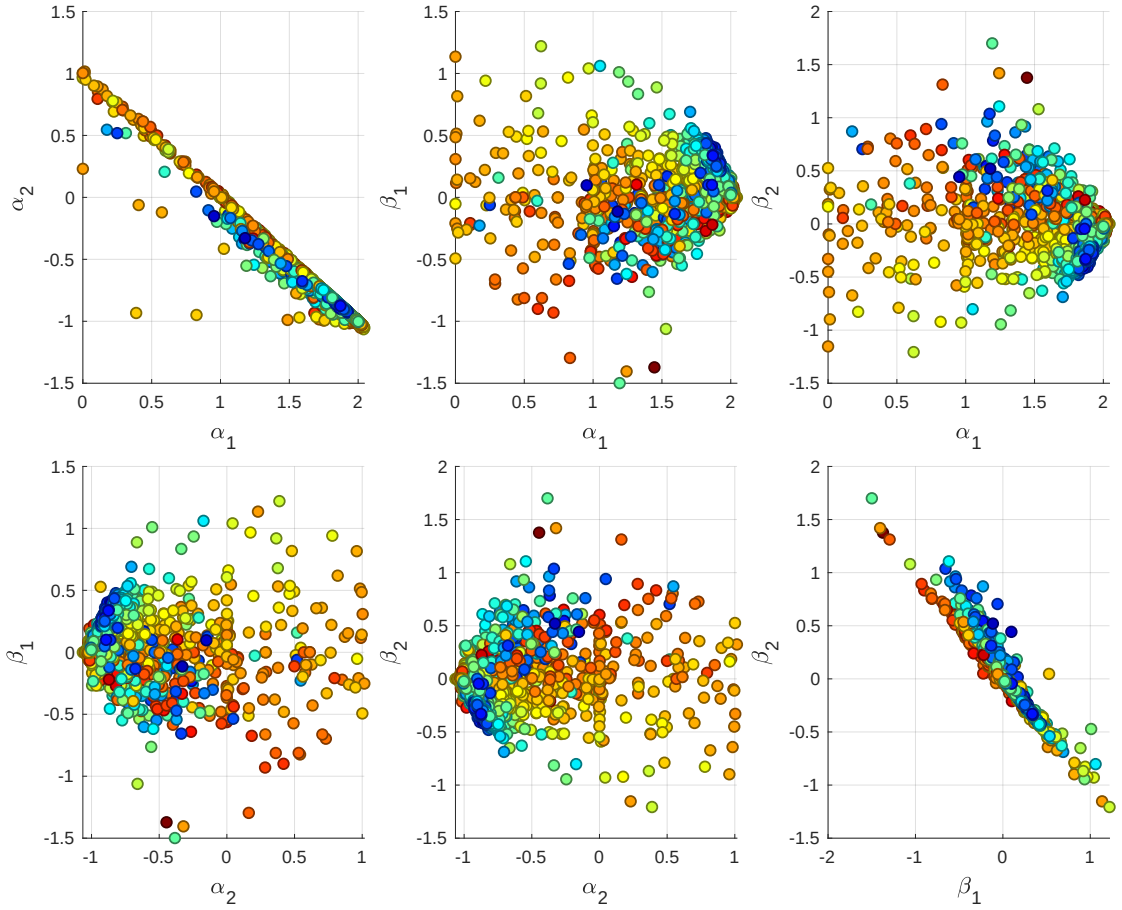

Figure 7: Parameter space of method S for arteries. Color temperature correlates with the distance from the golden average.

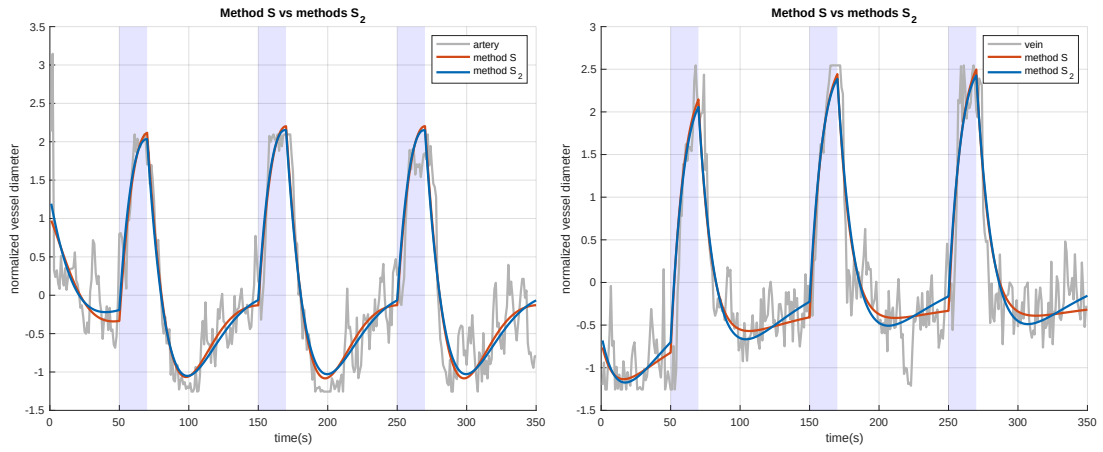

(a) artery (b) vein

Figure 8: Comparison of methods S and S_2 on an arbitrary artery and vein.

Notes on second order dynamics

The transfer function for Equation 15 is given by

$$H(z) = \frac{Y(z)}{U(z)} = \frac{\beta_1 + \beta_2 z^{-1}}{1 - \alpha_1 z^{-1} - \alpha_2 z^{-2}} = \frac{\beta_1 z^2 + \beta_2 z}{z^2 - \alpha_1 z - \alpha_2} = \frac{A_1 z}{z - d_1} + \frac{A_2 z}{z - d_2}, z \in \mathbb{C}, \tag{20}$$

with poles

$$d_{1,2} = \frac{\alpha_1 \pm \sqrt{\alpha_1^2 + 4\alpha_2}}{2}. \tag{21}$$

A_1 and A_2 can be calculated using partial fraction expansion resulting in

$$A_1 = \frac{\beta_1 d_1 + \beta_2}{d_1 - d_2} \text{ and } A_2 = \frac{\beta_1 d_2 + \beta_2}{d_2 - d_1}. \tag{22}$$

Therefore the impulse response of the system is

$$h(n) = A_1 d_1^n + A_2 d_2^n, \ \forall n \in \mathbb{N}_+. \tag{23}$$

Simplifications $\alpha_2 = c_1\alpha 1 + c_2$ and $\beta_2 = -\beta_1$ turn the poles and the impulse response into

$$d_{1,2} = \frac{\alpha \pm \sqrt{\alpha^2 + 4(\alpha c_1 + c_2)}}{2} = \frac{\alpha \pm \sqrt{\Delta}}{2}, \text{ and} \tag{24}$$

$$h(n) = \beta \frac{d_1 - 1}{\sqrt{\Delta}} d_1^n + \beta \frac{1 - d_2}{\sqrt{\Delta}} d_2^n. \tag{25}$$

Despite the simplifications, S_2 exhibits a rich dynamics. Similarly to the first order case, β influences the vertical orientation and the magnitude of the model response. Negative, or close to zero βs result in upside-down responses or small amplitude responses, both matching pathological measurements (e.g. Figure 4e).

For the impulse response to converge $||d_1||$ and $||d_2||$ must be bound by one (see Figure 9). $||d_1||$ is monotonically decreasing until the smaller root of Δ, $\Delta_0 = -2c_1 - 2\sqrt{c_1^2 - c_2}$ after which point d_1 becomes complex. Starting from Δ_0, $||d_1||$ is monotonically increasing and it reaches 1 at $\alpha = \frac{c_2 + 1}{-c_1}$. $||d_2||$ first reaches 1 at $\alpha = \frac{1 - c_2}{c_1 - 1}$, while monotonically decreasing until the inflection point at $\alpha = -\frac{c_2}{c_1}$. Afterwards it monotonically increases until the larger root of $\Delta_1 = -2c_1 + 2\sqrt{c_1^2 - c_2}$. $||d_2||$ reaches 1 second time at $\alpha = \frac{c_2 + 1}{-c_1}$. The impulse response $h(n)$ therefore converges if $\alpha \in \left(\frac{1 - c_2}{c_1 - 1}, \frac{c_2 + 1}{-c_1}\right)$.

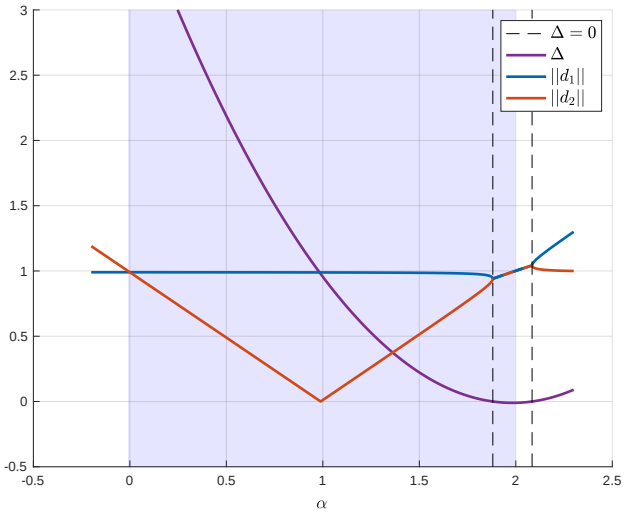

Figure 9: Convergence of the impulse response for arteries. The shaded area marked by $\alpha \in (-0.009, 2.084)$ is the region where both $||d_1||$ and $||d_2||$ are bound by 1.

Visualization

The parameter space of method S_2 shown in Figure 10. The plot resembles more the first order parameter space from Figure 4 than any of the pairwise plots in Figure 7. Although method S_2 α overflows the convergence boundaries to a greater extent, the reason is the same, i.e. capturing the trend present in the vessel measurement.

Discussion

Table 3 summarizes the main characteristics of the methods we have presented in the previous sections. Out of the five, two methods deserve to be mentioned again: the first order P and the second order S_2.

First order method P is intriguing because of the even spread of its parameters' map, and the smooth transition of the measurements' distances to the golden average (shown by the dots' colors) compared to the rest of methods. At the moment we do not know whether this linkage is genuine or some artifact. If it were genuine then the overshoot and recovery periods would loose considerably from their perceived significance, something which is difficult to accept form physiological point of view.

Method S_2 is interesting because of the context it emerged from: the strong and unexpected correlations among coefficients of method S. Though it is a full-blown second order method, S_2 depends only on two parameters, a compromise which brings better visualization of its parameters' map at the expense of increased modeling error. Loosely speaking, method S_2 is *barely* a second order model, as one of its poles, d_1 has a very flat, close-to-one norm in the range that interests us

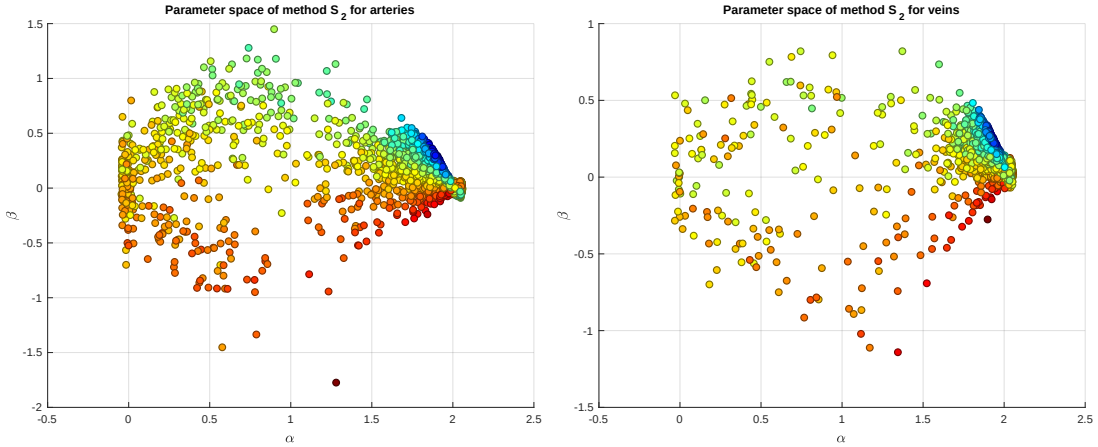

(a) arteries (b) veins

Figure 10: Parameter space of method S_2. Color temperature correlates with the distance from the golden average.

(see Figure 9).

Conclusions

In this paper we introduced first and second order models for the retinal flicker response, as recorded by DVA. We shown that second order difference equations are a good candidates, capturing all major aspects of the response. We have also shown that S_2, a two parameters, second order method is an attractive alternative for mapping the measurements into two dimensions.

Acknowledgments

Work partially supported by European Union's Horizon 2020 program, grant number 703570. AMJ would like to thank David Lowe, Nimród Kutasi and Sándor Horváth for the helpful discussions.

References

[1] Matteo Aletti. "Mathematical modelling and simulations of the hemodynamics in the eye". PhD thesis. Université Pierre et Marie Curie (UPMC Paris 6), 2017.

[2] Matteo Aletti, Jean-Frédéric Gerbeau, and Damiano Lombardi. "A simplified fluid–structure model for arterial flow. application to retinal hemodynamics". In: *Computer Methods in Applied Mechanics and Engineering* 306 (2016), pp. 77–94.

Table 3: Summary of methods.

method	order	pros	cons	other
P	1	fast, even spread of parameters map	does not capture overshoot and recovery	does not capture trend
S	1	—	slow, does not capture overshoot and recovery	captures trend
P	2	fast	parameter space hard to interpret, sensitive to noise, does not capture overshoot and recovery	does not capture trend
S	2	captures overshoot and recovery	slow, parameter space hard to interpret	captures trend
S_2	2	captures overshoot and recovery, sports only two parameters	slow, mean squared error higher than for method S	captures trend

[3] Matteo Aletti, Jean-Frédéric Gerbeau, and Damiano Lombardi. "Modeling autoregulation in three-dimensional simulations of retinal hemodynamics". In: *Journal for Modeling in Ophthalmology* 1 (2015).

[4] Julia Arciero et al. "Theoretical analysis of vascular regulatory mechanisms contributing to retinal blood flow autoregulation". In: *Investigative ophthalmology & visual science* 54.8 (2013), pp. 5584–5593.

[5] Stephen Boyd and Lieven Vandenberghe. *Convex optimization*. Cambridge University Press, 2004.

[6] Steven L Brunton, Joshua L Proctor, and J Nathan Kutz. "Discovering governing equations from data by sparse identification of nonlinear dynamical systems". In: *Proceedings of the National Academy of Sciences* (2016).

[7] Paola Causin and Francesca Malgaroli. "A mathematical and computational model of blood flow regulation in microvessels: Application to the eye retina circulation". In: *Journal of Mechanics in Medicine and Biology* 15.02 (2015), p. 1540027.

[8] Luca Formaggia, Alfio Quarteroni, and Allesandro Veneziani. *Cardiovascular Mathematics: Modeling and simulation of the circulatory system*. Vol. 1. Springer Science & Business Media, 2010.

[9] Gerhard Garhöfer et al. "Use of the retinal vessel analyzer in ocular blood flow research". In: *Acta ophthalmologica* 88.7 (2010), pp. 717–722.

[10] G Garhöfer et al. "Reduced response of retinal vessel diameters to flicker stimulation in patients with diabetes". In: *British Journal of Ophthalmology* 88.7 (2004), pp. 887–891.

[11] G Garhöfer et al. "Response of retinal vessel diameters to flicker stimulation in patients with early open angle glaucoma". In: *Journal of glaucoma* 13.4 (2004), pp. 340–344.

[12] Giovanna Guidoboni et al. "Intraocular pressure, blood pressure, and retinal blood flow autoregulation: a mathematical model to clarify their relationship and clinical relevance". In: *Investigative ophthalmology & visual science* 55.7 (2014), pp. 4105–4118.
[13] Allvar Gullstrand. "The dioptrics of the eye". In: *Helmholtz's Treatise on Physiological Optics, JPC Southall, ed.(Optical Society of America, 1924)* (), pp. 351–352.
[14] Martin Hammer and Walthard Vilser. *Method for measuring the vessel diameter of optically accessible blood vessels*. US Patent 7,756,569. July 2010.
[15] Henner Hanssen et al. "Exercise-induced alterations of retinal vessel diameters and cardiovascular risk reduction in obesity". In: *Atherosclerosis* 216.2 (2011), pp. 433–439.
[16] Rebekka Heitmar et al. "Continuous retinal vessel diameter measurements: the future in retinal vessel assessment?" In: *Investigative ophthalmology & visual science* 51.11 (2010), pp. 5833–5839.
[17] Gerhard A Holzapfel and Ray W Ogden. "Constitutive modelling of arteries". In: *Proceedings of the Royal Society A: Mathematical, Physical and Engineering Sciences* 466.2118 (2010), pp. 1551–1597.
[18] Lars Jaeger and Holger Kantz. "Unbiased reconstruction of the dynamics underlying a noisy chaotic time series". In: *Chaos: An Interdisciplinary Journal of Nonlinear Science* 6.3 (1996), pp. 440–450.
[19] Konstantin E Kotliar et al. "Dynamic retinal vessel response to flicker in obesity: a methodological approach". In: *Microvascular research* 81.1 (2011), pp. 123–128.
[20] Lennart Ljung. *System Identification: Theory for the User*. Prentice Hall Information and System Sciences Series. Prentice Hall PTR, 1999.
[21] Mary EJ Lott et al. "Impaired retinal vasodilator responses in prediabetes and type 2 diabetes". In: *Acta ophthalmologica* 91.6 (2013), e462–e469.
[22] Monica R Metea and Eric A Newman. "Signalling within the neurovascular unit in the mammalian retina". In: *Experimental physiology* 92.4 (2007), pp. 635–640.
[23] Sae-Il Murtada, Martin Kroon, and Gerhard A Holzapfel. "A calcium-driven mechanochemical model for prediction of force generation in smooth muscle". In: *Biomechanics and modeling in mechanobiology* 9.6 (2010), pp. 749–762.
[24] Edgar Nagel, Walthard Vilser, and Ines Lanzl. "Age, blood pressure, and vessel diameter as factors influencing the arterial retinal flicker response". In: *Investigative ophthalmology & visual science* 45.5 (2004), pp. 1486–1492.
[25] Alan V Oppenheim and Ronald W Schafer. *Discrete-time signal processing*. Pearson Education, 2014.
[26] Samuel H Rudy et al. "Data-driven discovery of partial differential equations". In: *Science Advances* 3.4 (2017).
[27] Doreen Schmidl et al. "Gender differences in ocular blood flow". In: *Current eye research* 40.2 (2015), pp. 201–212.
[28] Alexander Schuster et al. "Simultaneous arterial calcium dynamics and diameter measurements: application to myoendothelial communication". In: *American Journal of Physiology-Heart and Circulatory Physiology* 280.3 (2001), H1088–H1096.
[29] Jin Yang et al. "The myogenic response in isolated rat cerebrovascular arteries: smooth muscle cell model". In: *Medical engineering & physics* 25.8 (2003), pp. 691–709.